Zero energy states at a normal-metal/cuprate-superconductor interface probed by shot noise

O. Negri,[1,2] M. Zaberchik,[1,2] G. Drachuck,[1] A. Keren,[1] and M. Reznikov[1,2]
[1]*Department of Physics, Technion–Israel Institute of Technology, Haifa, 3200003, Israel*
[2]*Solid State Institute, Technion–Israel Institute of Technology, Haifa, 3200003, Israel*

(Received 18 July 2017; revised manuscript received 5 February 2018; published 11 June 2018)

We report measurements of the current noise generated in the optimally doped, $x = 0.15$, Au-$La_{2-x}Sr_xCuO_4$ junctions. For high transmission junctions on a (110) surface, we observed a split zero-bias conductance peak (ZBCP), accompanied by enhanced shot noise. We observed no enhanced noise neither in low-transmission junctions on a (110) surface nor in any junction on a (100) surface. We attribute the enhanced noise to Cooper pair transport through the junctions.

DOI: 10.1103/PhysRevB.97.214504

I. INTRODUCTION

Since the seminal work of Andreev [1], it has been understood that the current through a normal metal-superconductor (NS) interface at voltages below the superconductive gap Δ and at zero temperature is carried by Cooper pairs. An electron impinging from the metal picks up a pair, leaving a hole behind, so the charge transmitted in a single event is $2e$. This current, being partitioned by the interface, should generate shot noise with effective charge $2e$ [2,3]. Despite this seemingly simple prediction, interface-partitioned Cooper pair shot noise was observed only recently [4] in a single channel wire connected to a BCS superconductor. Impurity-partitioned shot noise generated in a *normal diffusive metal* by Cooper pairs reflected from a transparent NS interface was observed much earlier in Refs. [5,6].

In a normal metal-BCS superconductor junction, the low-voltage probability of pair transmission is $\Gamma_p = \Gamma_e^2$, where Γ_e is the single-electron transmission probability through the junction interface. At a finite temperature, the Cooper pair current competes with the single-particle current (proportional to Γ_e) and for a sufficiently low-transmission junction, such that $\Gamma_e \ll \exp(-\Delta/k_BT)$, the single-electron transport dominates.

The situation changes dramatically for a superconductor with a momentum-dependent gap $\Delta(\mathbf{k})$. In the case $\Delta(-k_\perp) = -\Delta(k_\perp)$, where $k_\perp$ is the momentum component in the direction normal to the NS interface, surface states with energy around the middle of the superconductive gap are formed [7–9]. Tunneling into these states leads to a zero-bias conduction peak (ZBCP) with Γ_e-dependent width, observed in tunneling experiments on d-wave high-temperature superconductors (HTSC) [10,11]. Treatment, similar to the one of the BTK paper [12] for BCS superconductors, leads to a prediction [9] of perfect pair transmission ($\Gamma_p = 1$) at zero voltage. Based on this expectation, it was predicted that the current in ZBCP region would generate no shot noise [13,14]. Indeed, low-frequency spectral density of the shot noise at zero temperature is given [2,15,16] by: $S = 2qI(1 - \Gamma_{e,p})$, where $q = e$ for single-electron and $q = 2e$ for pair transport.

Papers [8,9,13,14] treat an ideal case of a translationally-invariant NS interface, at which carrier reflection is specular. In practice, however, reflection at an NS interface is diffusive. Moreover, the surface of a superconductor is far from being perfect—it contains oxygen vacancies as in the case of YBCO, or a native oxidized layer, or just a normal layer of HTSC with substantial impurity scattering. Such nonidealities destroy perfect pair transmission [17–19] and should lead to finite shot noise [20–22]. In the case of tunneling from a pointlike STM tip, in which ZBCP are often observed [10,11], the geometry is very far from planar, so it is hard to expect Γ_p to be close to unity. Indeed, the differential conductance of a zero-bias peak in STM experiments [10,11,23–25] is typically orders of magnitude below $4e^2/h$ expected for a single channel with the unit transmission. In what follows, we present shot noise measurements which indicate pair transport through high-transmission junction in the ZBCP voltage region, while for low-transmission junctions we see no ZBCP and charge e shot noise.

II. EXPERIMENTAL SETUP

We used NS junctions on a (110) plane of optimally doped ($x = 15\%$) $La_{2-x}Sr_xCuO_4$ (LSCO). The $\Delta(\mathbf{k})$ in LSCO, as in other cuprate materials, is of $d_{x^2-y^2}$ symmetry [26]. Therefore, for electrons incident on a (110) plane, $\Delta(-k_\perp) = -\Delta(k_\perp)$ and zero energy states (ZES) are formed for every direction of an incident electron. As a result, the differential conductance should exhibit ZBCP. Transport through ZES can be either due to Andreev reflection with charge $2e$ transferred in a single event, or due to a single-particle process, in which an electron coming from the normal metal picks up a pair from HTSC to enter ZES [18,20,21]. In addition, an electron can pass as a charge-e quasiparticle in the nodal [110] direction. We exploit shot noise sensitivity to transmitted charge to distinguish between these processes.

We used an experimental setup shown schematically in Fig. 1. Current fluctuations generated by a junction produce voltage fluctuations across the parallel RLC resonant circuit [27] at the front end of a cryogenic amplifier. The frequency f of the resonant circuit is determined by the inductance L of the coil and the capacitance C of the junction and the cables. We chose $f \approx 20$ MHz to compromise between $1/f$ noise of the junction and current noise of the amplifier, which scales

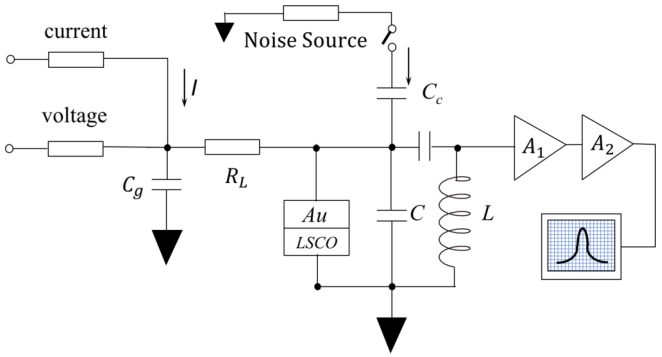

FIG. 1. The measurement circuit. A_1 and A_2 are the cryogenic and room-temperature amplifiers, respectively. DC current is driven through the load resistor R_L, the left-hand side of which is effectively grounded at RF frequencies through the capacitor C_g. Noise source was used for calibration at each value of the temperature and the current through a junction.

as f^2. The width of the resonance $\Delta f = 1/2\pi R_\parallel C$, where $R_\parallel^{-1} = R_{ac}^{-1} + R_L^{-1}$, depends on the load R_L and junction R_{ac} resistances at the resonance frequency. The signal from the cryogenic amplifier was fed into a room temperature one followed by a spectrum analyzer with a resolution bandwidth either 10 KHz or 100 KHz, depending on Δf. The resonant circuit, supplementary resistors, capacitors, and the cryogenic amplifier were mounted on the 2.7 K stage of a cryofree system inside a vacuum chamber. The sample box was anchored to the stage with a heat sink, weak enough to allow sample heating without significantly affecting the stage temperature. The sample box temperature was measured with a calibrated diode. The components of the measurement circuit were mounted inside a copper cage to minimize pickup noise. For noise measurements and calibration, we used semirigid coaxial cables.

We prepared the NS junctions by sputtering gold on first mechanically and then chemically polished surface of LSCO single crystals. Such a surface is covered by a natural insulating layer, which serves as a barrier. We defined 50×50 μm^2 gold pads by lithography and contacted them with wire bonds. Gold, sputtered on the back side of the samples and annealed at 500 °C, served as the ground contact. We measured a low-frequency differential conductance $G_{dc} = dI/dV$ typically at 77 Hz. The differential conductance G_{ac} at the frequency of the noise measurements was obtained from the width of the resonance; it happened to be higher than G_{dc} by about 10–15%, depending on the junction resistance. This discrepancy was important for proper calibration of the noise source, which was done against the thermal noise of the junction, similarly to Ref. [27].

III. EXPERIMENTAL RESULTS

In Fig. 2(a) we show G_{dc} against the voltage applied to the superconductor for a low-transmission junction J1 on a (110) surface and in Fig. 2(b) the noise generated by it. As prepared, the junction did not show a zero-bias conductance peak due to low transmission, $\Gamma_e \ll 1$. The differential conductance was V shaped, and the noise generated by the junction agreed well

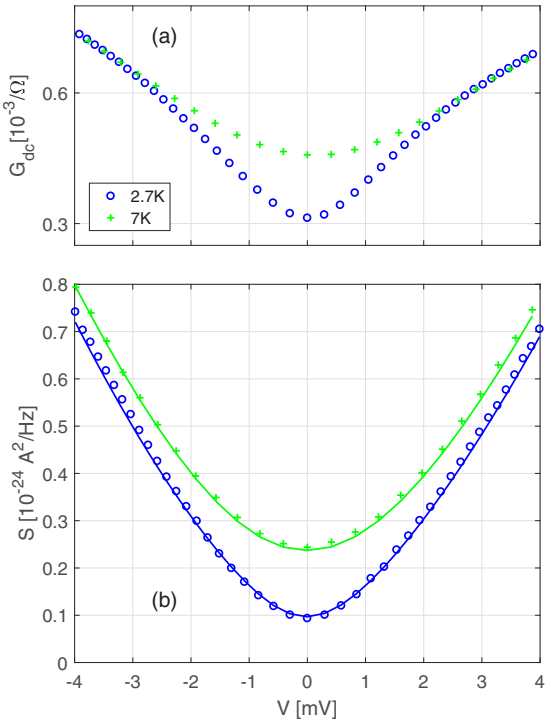

FIG. 2. (a) Differential conductance of a low-transmission $La_{2-x}Sr_xCuO_4$ junction J1. The G_{dc} is V shaped and the noise in panel (b) is fitted well with charge e, Eq. (1).

with the prediction [28,29] shown by solid line:

$$S_0 = 2qI\coth(qV/2k_BT) \tag{1}$$

with charge $q = e$ and no fitting parameter. Note that Eq. (1) is valid even for a junction with nonlinear current-voltage characteristic, provided the transmission probability through the barrier is small.

In order to improve transmission we, following Ref. [30], created pinholes in the surface barrier by discharging a 220 nF capacitor, charged to a voltage V_c, through a cold junction. The resistance of the junction would decrease with increasing V_c until, eventually, it would jump up and could not be further decreased. We considered such a junction as being burnt.

Below we present experimental results for junctions J2 and J3, which generate shot noise above the maximal one possible for charge e transport. In these junctions the transmission through the barrier was increased by discharge, so that inequality $\Gamma \ll 1$ used to derive Eq. (1) is no longer valid. This is apparent from the noise generated by these junctions at $eV \gg k_BT$, which for a low transmission junction according to Eq. (1) is expected to be temperature-independent *when plotted against current*. We plotted in Fig. 3 $S(I)$ for junctions J1–J3. At large currents (and large voltages as a result) the noise generated by junction J1 is temperature independent. This is the fingerprint of a small transmission probability through the barrier ($\Gamma \ll 1$). In contrast, at large currents the noise generated by junctions J2 and J3 is temperature dependent, indicating relatively large transmission probability. This can also be seen from the differential Fano factor $F = (1/2e)dS/dI$ at $eV \gg k_BT$, which should be unity for a low

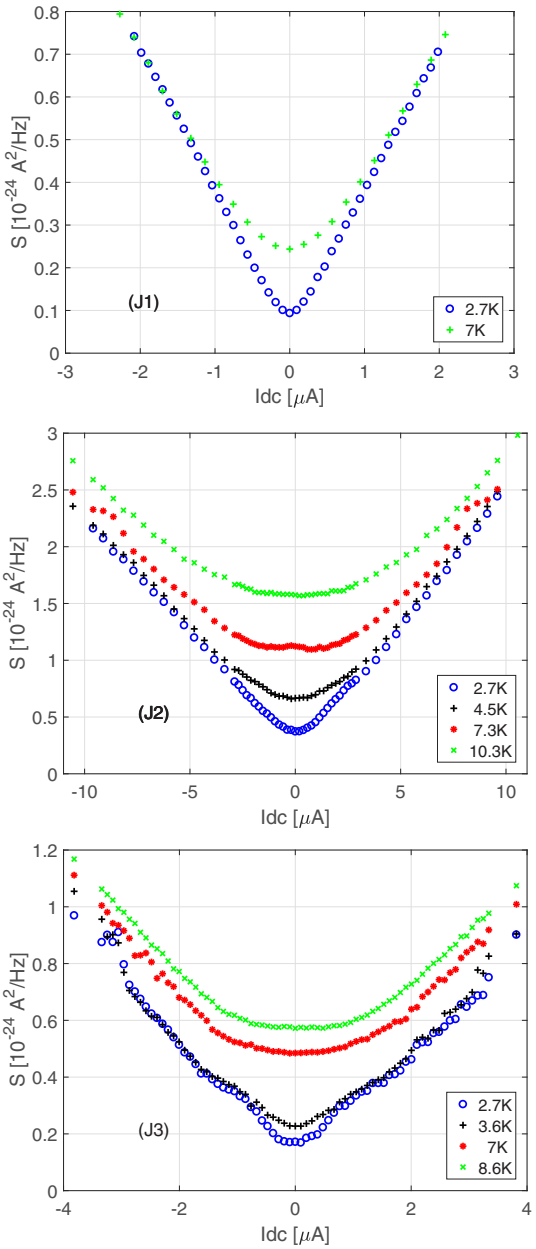

FIG. 3. Noise generated by samples J1, J2, J3 plotted as a function current. The current scale is different for different junctions due to their different resistance, the voltage span is the same: ±4 mV.

transmission junction, see Eq. (1), and should reduce with transmission: it is $1-\Gamma$ for a single channel with transmission Γ [16,31]. For junctions J2 and J3 the Fano factor $F \approx 0.6$ is significantly smaller than one.

In Figs. 4 and 5 we plot against voltage the conductance and noise generated by junctions J2 and J3. The conductance, although different in shape, exhibit ZBCP, which is slightly split in J2 and much strongly in J3; the ZBCPs disappear well below the bulk $T_c \approx 35$ K.

Due to high transmission of junctions J2 and J3, Eq. (1) cannot be used to predict the shot noise. Therefore, we chose to compare the observed noise with Eq. (2) which is a generalization of the prediction [32] derived for noninteracting electrons with *energy-independent finite* transmission through

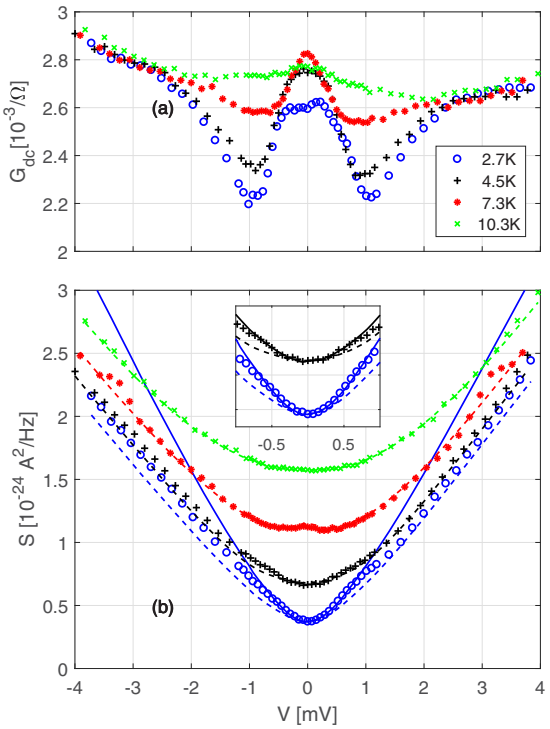

FIG. 4. (a) Differential conductance of junction J2 after discharge at 80 V. The ZBCP and minima on its sides are suppressed with heating at temperatures much smaller than the bulk T_c. (b) Experimental results for the noise S. Dashed lines are the fit $S_{\tilde{\Gamma}}$ from Eq. (2) with $q = e$ and temperature-independent $\tilde{\Gamma} = 0.4$ for $V < 0$ and 0.3 for $V > 0$. Solid lines—the maximal possible single-electron generated shot noise S_0. Inset: low voltage blowup. The fitting parameter $\tilde{\Gamma}$ is chosen to match the slope of the noise voltage dependence at large voltages.

the barrier:

$$S_{\tilde{\Gamma}} = 2qI(1-\tilde{\Gamma})\coth\left(\frac{qV}{2k_BT}\right) + 2k_BT\tilde{\Gamma}(G(0)+G(V)). \tag{2}$$

Here $\tilde{\Gamma} = \langle\Gamma_i(E)^2\rangle/\langle\Gamma_i(E)\rangle$, and $\Gamma_i(E)$ is the transmission probability through the barrier for channel i at energy E; Eq. (2) differs from the respective formula in Ref. [32] by Γ replaced with $\tilde{\Gamma}$. Equation (2) was derived in the Appendix under the assumptions of (i) energy-independent $\tilde{\Gamma}$ and (ii) independent transmission of particles through different channels and at different energies.

Equation (2) does not have the generality of Eq. (1). Still it: (i) reduces to the exact one for noninteracting electrons and energy-independent Γ_i, (ii) gives correct temperature dependence for energy-independent Γ_i at $eV \gg k_BT$, (iii) has correct zero-voltage ($4k_BTG$) and low-transmission [$\tilde{\Gamma} \to 0$, Eq. (1)] limits. In addition, charge enters into it exactly the same way as in Eq. (1), and thus it correctly captures charge doubling due to Andreev reflection in the $\Gamma_p \ll 1$ limit [2,3,28,29].

In Fig. 4(b) we show the noise generated by junction J2; for comparison we plot by the dashed line the expectation $S_{\tilde{\Gamma}}$ from Eq. (2) using $q = e$. We used $\tilde{\Gamma} = 0.4$ (corresponding to $F = 0.6$) for $V > 0$ and $\tilde{\Gamma} = 0.3$ ($F = 0.7$) for $V < 0$ to fit the *slope* of the data at large voltages, at which the

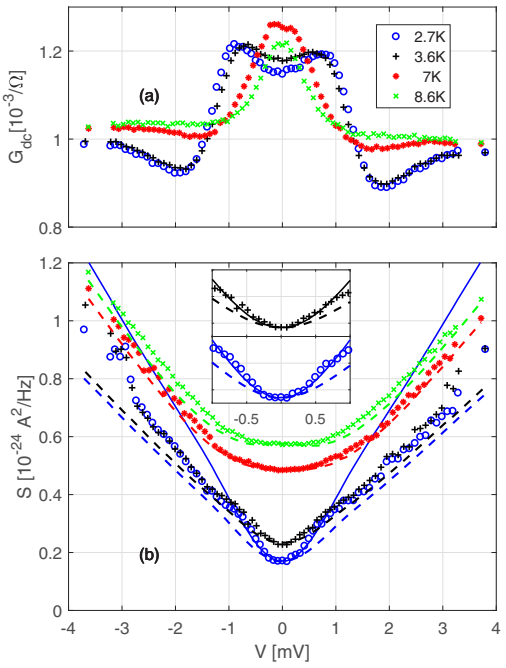

FIG. 5. (a) Differential conductance and (b) noise for junction J3 after discharge at 70 V; notations are the same as in Fig. 4. In this junction ZBCP is twice wider than in J2 and pronouncedly split. For this junction $\tilde{\Gamma}$ is temperature dependent: $\tilde{\Gamma} = 0.4,0.4,0.2,0.15$ for $V < 0$ and $0.45,0.45,0.3,0.25$ for $V > 0$ at temperatures from the lowest to the highest, respectively.

transmission is, presumably, constant. The data for this sample could be reasonably fit with temperature-independent $\tilde{\Gamma}$. Still, due to the assumptions made in the derivation of Eq. (2), the dashed lines in Figs. 3 and 4 should be considered only as a visual guide for the experimental results. At temperatures $T =$ 10.3 K and 7.3 K the fit is good; it even reproduces the small maximum at $V = 0$ due to enhanced thermal noise at ZBCP. At lower temperatures, and voltages below 1 mV, the experimental data lies above the expectation for $S_{\tilde{\Gamma}}$, with largest deviation at the lowest temperature of 2.7 K. The observed enhanced noise coincides with the *maximal possible* noise S_0 [shown in Fig. 4(b) by the solid line] expected for charge-e carriers from Eq. (1) [or Eq. (2) with $\tilde{\Gamma} = 0$].

In Fig. 5 we show results for another junction, J3, in which we observed a maximal enhancement of the low-temperature low-voltage noise above $S_{\tilde{\Gamma}}$ of all the measured samples. In this junction, ZBCP is twice wider than in J2 and pronouncedly split. Although both the conductivity and the noise generated by this sample behave somewhat differently with voltage and temperature, the low-temperature low-voltage behavior of the noise is similar: it exceeds S_0, and its low-voltage curvature is more than twice bigger than the curvature of $S_{\tilde{\Gamma}}$ and is 20% bigger than the curvature of S_0, both with charge $q = e$.

IV. DISCUSSIONS

The noise S in excess of S_0 cannot be attributed to the single-electron transport. Even $S = S_0$ requires transmissions of all junction's channels to be much smaller than unity, which clearly contradicts both the high-voltage slope and the temperature dependence of the observed noise. We, therefore, conclude that at low voltages at least a part of the current is carried by pairs which cross the barrier through Andreev reflection; the rest is due to the single-particle transport. We would like to emphasize that this conclusion does not rely on Eq. (2).

Most of the pair contribution is accumulated in the ZBCP region, below the voltage $|V| < 1$ mV. Above this voltage the noise increases roughly as predicted by Eq. (2) with $q = e$. In junction J2 at $T = 2.7$ K the pair contribution seems to survive at higher voltages, at least at $V < 0$, and disappears with temperature. In junction J3 at low temperatures and at voltages above ∼1.5 mV an additional, non-Gaussian source of noise starts to contribute. The rapid increase of the noise at $V < -1.5$ mV and increased scattering of the data points are indications of this.

Naively, ZBCP implies pair transmission through the barrier. This is, however, not necessarily the case: an electron passing through the barrier can entry ZES by pairing with an unpaired above-the-gap one from the superconductor itself, instead from the normal metal [18,20,21]. This process competes with Andreev reflection, the probability ratio between these processes being controlled by the parameter $\eta/\Gamma\Delta_0$, where η is the decay rate of ZES into the bulk of the superconductor, and Δ_0 is the maximal superconductive gap [18]. Let us consider what happens with an increase of the decay rate. The ideal case ($\Gamma_p = 1$) corresponds to $\eta = 0$; the current is due to Andreev reflection only ($q = 2e$), and it generates no shot noise. With an increase of η, Γ reduces and pair-generated shot noise appears. Simultaneously, a probability to pair with an electron from the superconductor also increases, so the noise due to the tunneling into ZES is generated by both charge e and $2e$. Since the gap is zero in d-wave superconductors, there is always a probability for an electron to pass into above-the-gap quasiparticle states; this process also generates a charge–e noise. As a result, one should not expect to see shot noise due to Andreev reflection only.

This above-the-gap quasiparticle current is also the reason why a junction at a (100) plane is a bad candidate for observation of Andreev reflection-enhanced noise, despite the superconductive gap being maximal in the [100] direction. In the absence of the peculiar interference which lead to significantly enhanced transmission in the [110] direction and to ZBCP, the transmission probability for pairs in a [100] direction is small, $\Gamma_p = \Gamma_e^2$, and the single-particle transport dominates. In agreement with expectations, we observe no ZBCP in junctions on a (100) surface of the optimally doped $La_{2-x}Sr_xCuO_4$. The observed shot noise agrees well with the prediction for single-electron transport since, in the absence of transmission enhancement leading to ZBCP, Andreev reflection is strongly suppressed.

Finally, we want to address other possible sources of excess noise. Since we measure noise at a relatively high frequency of ∼20 MHz and at low temperatures, the structure-related noise, such as a motion of impurities or their recharging, is very unlikely. One of the possibilities could be related to a subdominant order parameter, which can exist at a (110) surface due to the inversion symmetry breaking, which induces suppression of the bulk $\Delta_{x^2-y^2}$ order parameter [33–35]. This mechanism was proposed to explain ZBCP splitting [35].

Switching the subdominant order parameter on and off by large enough current can be a source of non-Gaussian excess noise. An alternative explanation for ZBCP splitting invokes fractional vortices on a (110) surface [36]. A current-induced motion of these vortices can be another source of non-Gaussian noise. We think that the above-mentioned mechanism can be responsible for the non-Gaussian noise at large currents in J3 [37].

To conclude, in high-transmission junctions on a (110) surface in the zero bias conduction peak region we observed enhanced shot noise due to pair transport through Andreev reflection. No enchanted noise was observed in low-transmission junctions, or in junctions on a (100) surface.

ACKNOWLEDGMENTS

We thank D. Podolsky and A. Auerbach for discussion. This work was supported by the Israeli Science Foundation.

APPENDIX: DERIVATION OF EQ. (2)

Below, we present a detailed derivation of Eq. (2) for the thermal and shot noise generated by electrons partitioned by a barrier [38]. We also argue that it is possible to judge about presence or absence of the high-transmission channels in a junction by looking at the temperature dependence of the noise only, without the assumption of energy-independent $\tilde{\Gamma}$ made in the derivation of Eq. (2). Let us consider a multichannel junction separated by a barrier with energy and channel-dependent transmissions $\Gamma_n(E)$. Assuming no correlation between different channels and at different energies, the current through the junction can be written as:

$$I = \frac{e}{h}\int dE \sum_n \Gamma_n(f_L(1-f_R) - f_R(1-f_L)) \quad \text{(A1)}$$

$$f_L = f_0((E-eV)/k_BT) \;\; f_R = f_0(E/k_BT). \quad \text{(A2)}$$

Here $f_0(x)$ is the Fermi distribution functions, and V is the voltage across the barrier; we do not indicate explicitly energy dependence of the variables under integrals for shortness. We assumed that the chemical potential is pinned on the right, superconductor, side of the barrier, which is a reasonable assumption for a native oxide on a sample.

In order to calculate low-frequency spectral density of the noise, we shall start with Eq. (61) of Ref. [32], which can be written as a sum of two terms $S = S_1 + S_2$:

$$S_1 = \frac{2e^2}{h}\int dE \sum_n \Gamma_n(1-\Gamma_n) \times (f_L(1-f_R) + f_R(1-f_L)) \quad \text{(A3)}$$

$$S_2 = \frac{2e^2}{h}\int dE \sum_n \Gamma_n^2(f_L(1-f_L) + f_R(1-f_R)). \quad \text{(A4)}$$

At $eV \gg k_BT$ the term S_1 is almost temperature independent and can be loosely viewed as shot noise; the term S_2 is proportional to the temperature and constitutes the thermal contribution to the noise. At low voltages, there is no such a distinction; at zero voltage $f_L = f_R$ and we recover the Johnson-Nyquist noise:

$$S_{JN} = \frac{4e^2}{h}\int dE \sum_n \Gamma_n f_L(1-f_L) = 4G(0)k_BT, \quad \text{(A5)}$$

where G(0) is the zero-voltage conductance. Here and below we assume that Γ's change little on the energy scale of the temperature, so df_0/dT can be replaced with δ function. Already from Eqs. (A4) and (A5) one can see that the ratio between the thermal contribution to the noise at $eV \gg k_BT$ and at $V = 0$ is equal to:

$$\sum_n \left(\Gamma_n^2(eV) + \Gamma_n^2(0)\right)/2 \sum_n \Gamma_n(0) = (\tilde{\Gamma}(eV) + \tilde{\Gamma}(0))/2. \quad \text{(A6)}$$

Here we defined:

$$\tilde{\Gamma}(E) = \sum_n \Gamma_n^2(E) / \sum_n \Gamma(E). \quad \text{(A7)}$$

Importantly, this ratio is small when all Γ_n are small, and the temperature-dependent high-voltage noise is indicative of high transmission through at least some channels.

To proceed, we observe that $f_R(1-f_L) = e^{-eV/k_BT} f_L(1-f_R)$, and therefore the expressions for I and S_1 would be very similar, if not for the factor $1-\Gamma_n(E)$ in S_1. Now Eqs. (A1) and (A3) can be written as:

$$I = \frac{e}{h}\int dE \sum_n \Gamma_n f_L(1-f_R)(1-e^{-eV/k_BT}) \quad \text{(A8)}$$

$$S_1 = \frac{2e^2}{h}\int (1-\tilde{\Gamma}) dE \sum_n \Gamma_n f_L(1-f_R)(1+e^{-eV/k_BT}). \quad \text{(A9)}$$

If we assume $\tilde{\Gamma}$ to be energy independent, we can take it out of the integral and, comparing with Eq. (A8), arrive at a particularly simple expression:

$$S_1 = 2eI(1-\tilde{\Gamma})\coth(eV/2k_BT). \quad \text{(A10)}$$

For a low transmission junction, Eq. (A10) reduces to Eq. (1) of the paper with charge $q = e$. Similar treatment in the case of Andreev reflection would give for S_1 Eq. (A10) with charge $2e$.

Now, we shall relate S_2 with the voltage-dependent differential conductance $G(V)$ of the junction. Differentiating Eq. (A1) and assuming that the barrier, and therefore $\Gamma_n(E)$, are voltage independent we find:

$$G = \frac{e}{h}\sum_n \int dE \Gamma_n \frac{df_L}{dV}. \quad \text{(A11)}$$

Observing that $df_L/dV = (e/k_BT) f_0(x)(1-f_0(x))$ with $x = (E-eV)/k_BT$, and using Eq. (A7), we get for S_2:

$$S_2 = 2k_BT \sum_n \frac{e^2}{h}(\Gamma_n(0)(1-\Gamma_n(0)) + \Gamma_n(eV)(1-\Gamma_n(eV))$$
$$= 2k_BT(\tilde{\Gamma}(0)G(0) + \tilde{\Gamma}(eV)G(eV)). \quad \text{(A12)}$$

The term $G(0)$ comes from $f_R(1-f_R)$ in Eq. (A4). By this, we recover Eq. (2) of the paper with $q=e$. Note that in the case where the voltage is equally divided between the right and left sides of the barrier, we would get instead of Eq. (A12):

$$S_2 = 4k_BT\frac{e^2}{h}\sum_n \Gamma_n(eV)(1-\Gamma_n(eV)) = 4k_BT\tilde{\Gamma}(eV)G(eV). \tag{A13}$$

Fortunately, the difference between results (A12) and (A13) is very small for our junctions. Assuming energy-independent $\tilde{\Gamma}$ we recover Eq. (2) of the paper.

[1] A. F. Andreev, Sov. Phys. JETP **19**, 1228 (1964).
[2] V. K. Khlus, JETP **66**, 1243 (1987).
[3] B. A. Muzykantskii and D. E. Khmelnitskii, Phys. Rev. B **50**, 3982 (1994).
[4] A. Das, Y. Ronen, M. Heiblum, D. Mahalu, A. V. Kretinin, and H. Shtrikman, Nat. Commun. **3**, 1165 (2012).
[5] X. Jehl, P. Payet-Burin, C. Baraduc, R. Calemczuk, and M. Sanquer, Phys. Rev. Lett. **83**, 1660 (1999).
[6] B. Reulet, A. A. Kozhevnikov, D. E. Prober, W. Belzig, and Y. V. Nazarov, Phys. Rev. Lett. **90**, 066601 (2003).
[7] C. Bruder, Phys. Rev. B **41**, 4017 (1990).
[8] C.-R. Hu, Phys. Rev. Lett. **72**, 1526 (1994).
[9] Y. Tanaka and S. Kashiwaya, Phys. Rev. Lett. **74**, 3451 (1995).
[10] A. Sharoni, O. Millo, A. Kohen, Y. Dagan, R. Beck, G. Deutscher, and G. Koren, Phys. Rev. B **65**, 134526 (2002).
[11] A. Sharoni, G. Leibovitch, A. Kohen, R. Beck, G. Deutscher, G. Koren, and O. Millo, Europhys. Lett. **62**, 883 (2003).
[12] G. E. Blonder, M. Tinkham, and T. M. Klapwijk, Phys. Rev. B **25**, 4515 (1982).
[13] J.-X. Zhu and C. S. Ting, Phys. Rev. B **59**, R14165(R) (1999).
[14] Y. Tanaka, T. Asai, N. Yoshida, J. Inoue, and S. Kashiwaya, Phys. Rev. B **61**, R11902 (2000).
[15] G. B. Lesovik, JETP Lett. **49**, 592 (1989).
[16] B. Yurke and G. P. Kochanski, Phys. Rev. B **41**, 8184 (1990).
[17] A. Golubov and M. Kupriyanov, Superlattices Microstruct. **25**, 949 (1999).
[18] T. Löfwander, V. S. Shumeiko, and G. Wendin, Supercond. Sci. Technol. **14**, R53 (2001).
[19] Y. Tanaka, A. A. Golubov, and S. Kashiwaya, Phys. Rev. B **68**, 054513 (2003).
[20] T. Löfwander, V. S. Shumeiko, and G. Wendin, Physica C **367**, 86 (2002).
[21] T. Löfwander, M. Fogelström, and J. A. Sauls, Phys. Rev. B **68**, 054504 (2003).
[22] P. Burset, B. Lu, S. Tamura, and Y. Tanaka, Phys. Rev. B **95**, 224502 (2017).
[23] T. Kato, S. Okitsu, and H. Sakata, Phys. Rev. B **72**, 144518 (2005).
[24] T. Kato, T. Maruyama, S. Okitsu, and H. Sakata, J. Phys. Soc. Jpn. **77**, 054710 (2008).
[25] S. H. Pan, J. O'neal, R. Badzey, C. Chamon, H. Ding, J. Engelbrecht, Z. Wang, H. Eisaki, S. Uchida, A. Gupta *et al.*, Nature (London) **413**, 282 (2001).
[26] We use here the standard axes designation with x, y and z being in the a, b, and c directions, respectively.
[27] R. De-Picciotto, M. Reznikov, M. Heiblum, V. Umansky, G. Bunin, and D. Mahalu, Physica B **249**, 395 (1998).
[28] D. Rogovin and D. J. Scalapino, Ann. Phys. **86**, 1 (1974).
[29] L. S. Levitov and M. Reznikov, Phys. Rev. B **70**, 115305 (2004).
[30] Y. Dagan, A. Kohen, G. Deutscher, and A. Revcolevschi, Phys. Rev. B **61**, 7012 (2000).
[31] G. Lesovik, ZhETF Pisma Redaktsiiu **49**, 513 (1989).
[32] Y. M. Blanter and M. Buttiker, Phys. Rep. **336**, 1 (2000).
[33] M. Matsumoto and H. Shiba, J. Phys. Soc. Jpn. **64**, 4867 (1995).
[34] M. Sigrist, D. B. Bailey, and R. B. Laughlin, Phys. Rev. Lett. **74**, 3249 (1995).
[35] M. Fogelström, D. Rainer, and J. A. Sauls, Phys. Rev. Lett. **79**, 281 (1997).
[36] P. Holmvall, A. B. Vorontsov, M. Fogelström, and T. Löfwander, arXiv:1711.07946.
[37] We observed strong non-Gaussian noise in some samples (unpublished).
[38] We define the spectral density for the positive frequencies only.